International Journal of Current Engineering and Technology
ISSN 2277 - 4106

Available at http://inpressco.com/category/ijcet

Research Article

Elaboration and Characterization of Alumina-Tricalcium Phosphate Composites

Siwar Sakka [Å*], Jamel Bouaziz [Å] and Foued Ben Ayed [Å]

[Å] Laboratory of Industrial Chemistry , National School of Engineering, *Box 1173, 3038 Sfax*, University of Sfax, Tunisia

Accepted 25 November 2013, Available online 01 December 2013, **Vol.3, No.5 (December 2013)**

Abstract

The effect of β-tricalcium phosphate additive on the alumina matrix was investigated. The sintering behaviour of the alumina - tricalcium phosphate composites was characterized by using magic angle spinning nuclear magnetic resonance, X-ray diffraction, dilatometry, differential thermal analysis and scanning electron microscopy analysis. The mechanical properties of composites have been investigated by the Brazilian test. The produced alumina - tricalcium phosphate composites with different percentages of β- tricalcium phosphate (10 wt%; 20 wt%; 40 wt% and 50 wt%) exhibited much better mechanical properties than the reported values of β- tricalcium phosphate without alumina. The alumina - tricalcium phosphate composites showed a higher rupture strength at 1600°C, which certainly increased with the alumina content and reached the optimum value with 90 wt%. The best mechanical properties of the composites were obtained after the sintering process at 1600°C for 1 hour. With different weight rations of alumina: tricalcium phosphate (50:50, 60:40 and 80:20), the performance of the composites was hindered by the formation of both cracks and intragranular porosity.

Keywords: *Bioceramics, β- tricalcium phosphate, Alumina, Composites, Sintering, Mechanical properties.*

1. Introduction

Calcium phosphates (CaP) have been sought as biomaterials for reconstruction of bone defect in maxillofacial, dental and orthopaedic applications (Hench, L L. 1991; Hench, L L. 1993; Elliott, J C. 1994; Landi, E. *et al* 2000; Ben Ayed, F *et al* 2000, 2001; Destainville, A *et al* 2003; Gaasbeek, R D *et al* 2005; Jensen, S S *et al* 2006; LeGeros, R Z *et al* 1991). Calcium phosphates have been used clinically to repair bone defects for many years. Calcium phosphates such as hydroxyapatite ($Ca_{10}(PO_4)_6(OH)_2$, HAp), fluorapatite ($Ca_{10}(PO_4)_6F_2$, FAp), tricalcium phosphate ($Ca_3(PO_4)_2$, TCP), TCP-HAp composites and TCP-FAp composites are used for medical and dental applications (Elliott, J C. 1994; Gaasbeek, R D *et al* 2005; Jensen, S S *et al* 2006; Ben Ayed, F *et al* 2006, 2011; Guha, A K *et al* 2009; Tamai, N *et al* 2002; Chu, T M G *et al* 2002; Schnettler, R *et al* 2004).

The main reason behind the use of β-TCP as bone substitute materials is their chemical similarity to the mineral component of mammalian bone and teeth (Hench, L L. 1991, 1993; Elliott, J C. 1994). The application of tricalcium phosphate as a bone substitute has received considerable attention, because it is remarkably biocompatible with living bodies when replacing hard tissues and because it has biodegradable properties (Hench, L L. 1991, 1993; Elliott, J C. 1994, Landi, E. *et al* 2000; Ben Ayed, F *et al*., 2000, 2001; Destainville, A *et al* 2003; Gaasbeek, R D *et al* 2005; Jensen, S S *et al* 2006; Hoell, S *et al*, 2005; Langstaff, S D *et al* 2001). Consequently, β-TCP has been used as bone graft substitutes in many surgical fields such as orthopedic and dental surgeries (Elliott, J C. 1994; Hoell, S *et al*, 2005; Gaasbeek, R D *et al* 2005; Gutierres, M *et al* 2007; DeSilva, G L *et al* 2007). This use leads to an ultimate physicochemical bond between the implants and bone-termed osteointegration. Even so, the major limitation to the use of β-TCP as load-bearing biomaterial is their mechanical properties which make it brittle, with poor fatigue resistance (Elliott, J C. 1994; Wang, C X *et al* 2004; Bouslama, N *et al* 2009a, 2010; Guha, A K *et al* 2009; Ben Ayed, F *et al* 2011; Sellami, I *et al* 2012; Sakka, S *et al* 2012). Moreover, the mechanical properties of tricalcium phosphate are generally inadequate for many load-carrying applications (3 MPa – 5 MPa) (Elliott, J C. 1994; Wang, C X *et al* 2004; Ayed, F *et al* 2008; Bouslama, N *et al* 2009a; Guha, A K *et al* 2009; Sellami, I *et al* 2012; Sakka, S *et al* 2012). Its poor mechanical behaviour is even more evident when used to make highly porous ceramics and scaffolds. Hence, metal oxides ceramics, such as alumina (Al_2O_3), titania (TiO_2) and some oxides (e.g. ZrO_2, SiO_2) have been widely studied due to their bioinertness, excellent tribological properties, high wear resistance, fracture toughness and strength as well as relatively low friction (Ben Ayed, F *et al* 2008; Bouslama, N *et al* 2009b), Guidara, A *et al* 2011). However, bioinert

*Corresponding author: **Siwar Sakka**

ceramic oxides having high strength are used to enhance the densification and the mechanical properties of β-TCP. In this paper, we will try to improve the strength of β-TCP by introducing a bioinert oxide like alumina. This is because there are few articles reporting the toughening effects of an inert oxide (like alumina (Al_2O_3)) on the mechanical properties of β-TCP (Bouslama, N *et al* 2009b; S. Sakka et al., 2012). Alumina has a high strength and is bio-inert with human tissues (Ben Ayed, F *et al* 2008; Bouslama, N *et al* 2009b; Sakka, S *et al 2012*). In order to improve the biocompatibility of alumina and the strength of tricalcium phosphate effectively, and in order to search for an approach to produce high performances of alumina-tricalcium phosphate composites, β-TCP is introduced with different percentages in the alumina matrix. The aim of our study is to elaborate and characterize the TCP-Al_2O_3 composites for biomedical applications.

This paper proposes to study the sintering of the alumina-tricalcium phosphate composites at various temperatures (1400°C, 1450°C, 1500°C, 1550°C and 1600°C) and with different percentages of β-TCP (10 wt%, 20 wt%, 40 wt% and 50 wt%). The characterization of biomaterials will be realized by using dilatometry analysis, differential thermal analysis (DTA), X-ray diffraction (XRD), magic angle spinning nuclear magnetic resonance (MAS NMR), scanning electron microscopy analysis (SEM) and by using the mechanical properties, such as rupture strength (σ_r) of these biomaterials.

2. Materials and methods

The synthesized tricalcium phosphate and alumina (Riedel-de Haën) were mixed in order to prepare biomaterial composites. The β-TCP powder was synthesized by solid-state reaction from calcium carbonate ($CaCO_3$) and calcium phosphate dibasic anhydrous ($CaHPO_4$) (Sakka, S *et al 2012*). Stoichiometric amounts of high purity powders such as $CaHPO_4$ (Fluka, purity ≥ 99%) and $CaCO_3$ (Fluka, purity ≥ 98.5%), were sintered at 1000°C for one hour to obtain the β-TCP according to the following reaction:

$$2\,CaHPO_4(s) + CaCO_3(s) \rightarrow Ca_3(PO_4)_2(s) + H_2O(g) + CO_2(g) \quad (1)$$

The β-TCP and the alumina powders were mixed in an agate mortar. The powder mixtures were milled in ethanol for 24 hours. After milling, the mixtures were dried in a rotary vacuum evaporator and passed through a 70-mesh screen. After drying the powder mixtures at 80°C for 24 hours, they were molded in a cylinder having a diameter of 20 mm and a thickness of 6 mm, and pressed under 150 MPa. The green compacts were sintered at various temperatures for one hour in a vertical furnace (Pyrox 2408). The heating rate is 10°C min^{-1}. The size of the particles of the powder was measured by means of a Micromeritics Sedigraph 5000. The specific surface area (SSA) was measured using the BET method and using N_2 as an adsorption gas (ASAP 2010) (Brunauer, S. *et al* 1938). The primary particle size (D_{BET}) was calculated by assuming the primary particles to be spherical:

$$D_{BET} = 6 / S\,\rho \quad (2)$$

where ρ is the theoretical density and S is the surface specific area.

The microstructure of the sintered compacts was investigated using the scanning electron microscope (Philips XL 30) on the fractured surfaces of the samples. The grains mean size was measured directly using SEM micrographs. The powder was analyzed by using X-ray diffraction (XRD). The X-ray patterns were recorded using the Seifert XRD 3000 TT diffractometer. The X-ray radiance was produced by using CuK_α radiation (λ = 1.54056 Å). The crystalline phases were identified with the powder diffraction files (PDF) of the International Center for Diffraction Data (ICDD). Linear shrinkage was determined using dilatometry (Setaram TMA 92 dilatometer). The heating and cooling rates were 10°C min^{-1} and 20°C min^{-1}, respectively. Differential thermal analysis (DTA) was carried out using about 30 mg of powder (DTA-TG, Setaram Model). The heating rate was 10°C min^{-1}. The ^{31}P and ^{27}Al magic angle spinning nuclear magnetic resonance (^{31}P MAS NMR) spectra were run on a Brucker 300WB spectrometer. The ^{31}P and ^{27}Al observational frequency were 121.49 MHz and 78.2 MHz, respectively. The ^{31}P MAS-NMR chemical shifts were referenced in parts per million (ppm) referenced to 85 wt% H_3PO_4. The ^{27}Al MAS-NMR chemical shifts were referenced to a static signal obtained from an aqueous aluminum chloride solution.

The Brazilian test was used to measure the rupture strength of biomaterials, (ISRM, 1978; ASTM C496, 1984). The rupture strength (σ_r) values were measured using the Brazilian test according to the equation:

$$\sigma_r = \frac{2 \cdot P}{\Pi \cdot D \cdot t} \quad (3)$$

where P is the maximum applied load, D the diameter, t the thickness of the disc and σ_r the rupture strength (or mechanical strength).

3. Results and discussion

3. 1. Characterization of different powders

The X-ray diffraction analysis of β-TCP powder and α-alumina powder are presented in Fig.1. As it can be noticed from this figure, the X-ray diffraction pattern of tricalcium phosphate powder reveals only peaks of β-TCP (ICDD data file no. 70-2065) without any other phase (Fig. 1a). Consequently, the XRD pattern obtained from the alumina powder illustrates α phase peaks relative to ICDD data file no. 43-1484 (Fig. 1b).

The ^{31}P MAS-NMR solid spectrum of the tricalcium phosphate powder is presented in Fig. 2a. We observe the presence of several peaks of tetrahedral P sites (at 0.36 ppm, 1.46 ppm and 4.83 ppm), while there are other peaks (at -7.43 ppm, -9.09 ppm and -10.35 ppm) which reveal a

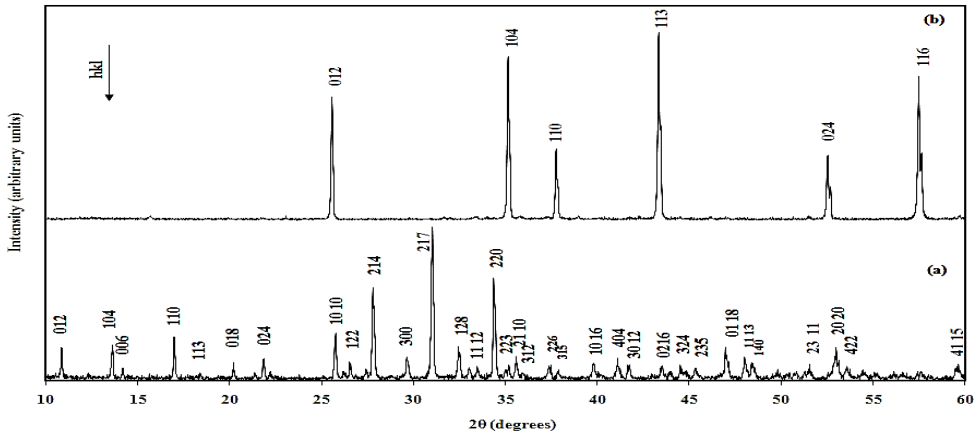

Fig. 1 The XRD patterns of: (a) β-TCP powder and (b) α-Al_2O_3 powder

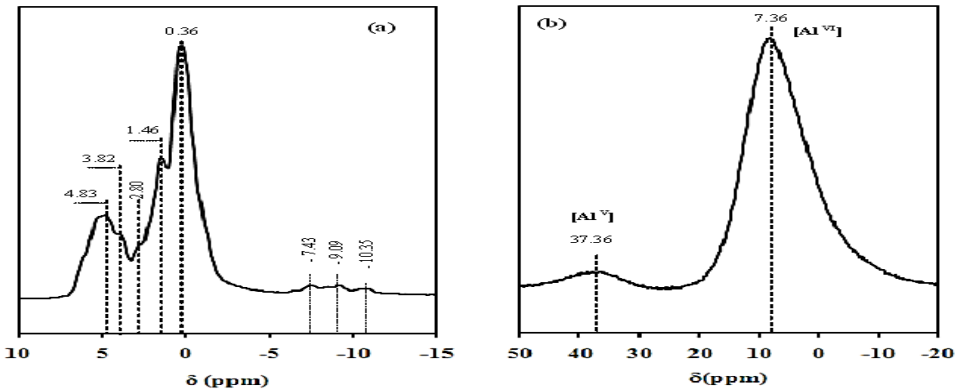

Fig 2 The ^{31}P MAS-NMR spectra of: (a) β-TCP and the ^{27}Al MAS-NMR spectra of: (b) α-Al_2O_3

Table 1 Characteristics of the powders used in the study

Compounds	SSA (m^2/g) ± 1.0	D_{BET} (µm) ± 0.2	D_{50} (µm)[a] ± 0.2	DTA measurements (endothermic peak)	T(°C)[b]	d[c]
TCP	0.7	2.79	6	1100°C-1260°C (β → α)	1000 - 1300	3.070 (β)
				1470°C (α → α')		2.860 (α)
Alumina	2.87	0.53	3	-	1400 - 1600	3.98 (α)

[a] : mean diameter, [b] : sintering temperature domain, [c] : theoretical density

low quantity of calcium pyrophosphate which was formed during the preparation of the β-TCP.

The ^{27}Al MAS-NMR solid spectrum of the alumina powder is presented in Fig. 2b. We notice the presence of two peaks which are characteristic of aluminum: one peak at 7.36 ppm corresponding to octahedral Al sites (Al^{VI}) and the other at 37.36 ppm which corresponds to pentahedral Al sites (Al^{V}). The results obtained for ^{31}P MAS-NMR and ^{27}Al MAS-NMR are similar to those previously reported by different authors (Ben Ayed, F *et al* 2006, 2011; Bouslama, N *et al* 2009b, 2010; Sakka, S *et al* 2012; Guidara, A *et al* 2011).

The experimental characteristics of the different powders used in this study are illustrated in Table 1. Table 1 summarizes the SSA, the DTA measurements, the sintering temperature and the theoretical density of the different powders. The powder particles are assumed to be spherical; the size of the particles can be calculated using Eq. (2). The results from the average grain size obtained by the SSA (D_{BET}) and from the average grain size obtained by granulometric repartition (D_{50}) are presented in Table 1. Compared with those of the β-TCP powder, the grains of the alumina powder have a dense morphology. These (DBET) values obtained by the SSA do not correspond to those obtained from the granulometric repartition (Table 1). The discrepancy may be due to the presence of agglomerates which are formed during the preparation of the β-TCP powder at 1000°C.

Differential thermal analysis studies of the different powders used in this study detected a potential phase change during the sintering process. The DTA thermogram of β-TCP, α-Al_2O_3 and different Al_2O_3 - TCP composites are presented in Fig. 3. The DTA curve of alumina reported no process relative to the sintering temperature (Fig. 3a). Fig. 3b shows the DTA curve of β-

TCP. The DTA thermogram of β-TCP shows two endothermic peaks, relative to the allotropic transformations of tricalcium phosphate (Fig. 3b). The peak between 1100°C – 1260°C is related to the first allotropic transformation of TCP (β to α), while the last peak at 1470°C is related to the second allotropic transformation of TCP (α to α'). As a matter of fact, this result is similar to the result previously reported by Destainville *et al.* and Ben Ayed *et al.* (Destainville, A *et al* 2003), Ben Ayed, F *et al* 2006). Fig. 3c shows the DTA curve of Al_2O_3-50 wt% TCP composites. This DTA curve is practically similar to the one shown in Fig. 3b. Indeed, the DTA thermogram of the composites also shows two endothermic peaks. Fig. 3 (d), (e) and (f) illustrate the DTA curves of Al_2O_3–40 wt% TCP composites, Al_2O_3–20 wt% TCP composites and Al_2O_3–10 wt% TCP composites, respectively. The DTA thermograms of each composites show only one endothermic peak between 1100°C and 1260°C, which are relative to the allotropic transformation of TCP (β to α). In these curves, we notice that the endothermic peak relative to a second allotropic transformation of TCP (α to α') has practically disappeared when the percentage of the alumina increases in the Al_2O_3 - TCP composites (Fig. 3(d), (e) and (f)).

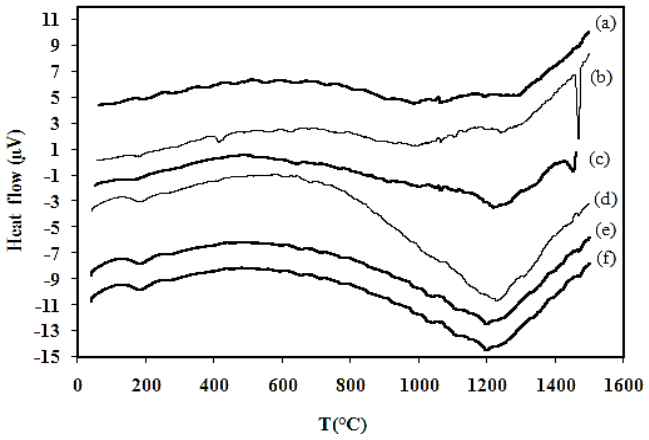

Fig. 3 DTA curves of (a) α-Al_2O_3, (b) β-TCP, (c) Al_2O_3 – 50 wt% TCP composites, (d) Al_2O_3 – 40 wt% TCP composites, (e) Al_2O_3 – 20 wt% TCP composites and (f) Al_2O_3 – 10 wt% TCP composites

Fig. 4 shows the dilatometric measurements of the different powders used in this study (β-TCP, α-Al_2O_3 and Al_2O_3 - TCP composites). A large sintering domain was observed for the three powders (β-TCP, alumina and composites). The sintering temperature of the initial powder began at about 900°C and at about 1400°C for the β-TCP and alumina (Fig. 4a-b and Table 2). The sintering temperature of Al_2O_3-50 wt% TCP composites began at 1100°C (Fig. 4c). It is to be noted that the presence of 50 wt% TCP in the alumina matrix decreases the sintering temperature of the alumina by around 300°C (Fig. 4c). This variation of the sinterability is relative to the difference between the physicochemical compositions of these powders and the mixture of their different composites.

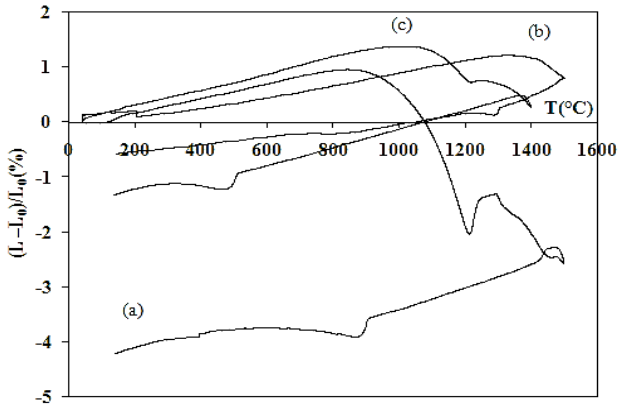

Fig 4 Linear shrinkage versus temperature of: (a) β-TCP, (b) α-Al_2O_3 and (c) Al_2O_3 – 50 wt% TCP composites

3. 2. The mechanical properties of alumina–tricalcium phosphate composites

The influence of the sintering temperature on the rupture strength of Al_2O_3-TCP composites is shown in Table 2. The mechanical resistance of Al_2O_3-TCP composites is studied at various temperatures (1400°C, 1450°C, 1500°C, 1550°C, 1600°C) for one hour with different percentages of β-TCP (50 wt%, 40 wt%, 20 wt% and 10 wt%). Thus, Table 2 illustrates the rupture strength of the Al_2O_3-TCP composites relative to the percentages of the alumina and the sintering temperature. Consequently, the rupture strength of Al_2O_3 mixed with 10 wt% β-TCP reached its maximum value when sintered at 1600°C for one hour; it then decreased with the increase of this percentage. This is how the rupture strength of the Al_2O_3-10 wt% TCP composites reached 13.5 MPa.

In this study, we showed that the presence of different amounts of alumina in the β-TCP improves the mechanical properties of Al2O3-TCP composites. In fact, the mechanical properties of Al2O3-10 wt% TCP composites reached the optimum value by being sintered at 1600°C for one hour. Thus, the rupture strength of these composites reached 13.5 MPa. Table 3 displays several examples of the mechanical properties of the calcium phosphates and the bone tissues. In comparison, we notice that the properties of Al2O3-10 wt% TCP composites are close to those of pure β-TCP, pure Fap and TCP-33.16 wt% Fap composites, which have a rupture strength of 5.3 MPa, 14 MPa and 13.7 MPa, respectively (Ben Ayed, F et al 2006), (Bouslama, N et al 2009a, 2010). However, the mechanical properties of our composites are more closely comparable to those of the pure Fap and the TCP–33.16 wt% Fap composites (Table 3). Generally, the values found for the mechanical strength of our composites are not identical to those in Table 3, because the authors have used different mechanical modes other than the Brazilian test. In addition, many factors influence the mechanical properties of the samples such as: the use of particular initial powders as well as the conditions of the treatment process.

The sintering of materials is a complex process, involving the evolution of the microstructure through the

Table 2 The rupture strength of the TCP-Al_2O_3 composites sintered for 1 hour at various temperatures: (a) 1400°C, (b) 1450°C, (c) 1500°C, (d) 1550°C and (e) 1600°C

Composites	Rupture strength σ_r (MPa)				
	1400°C	1450°C	1500°C	1550°C	1600°C
50 wt% TCP-Al_2O_3	1,60	2,24	2,96	3,97	5,82
40 wt% TCP-Al_2O_3	1,58	2,07	3,04	4,40	6,23
20 wt% TCP-Al_2O_3	1,93	2,54	3,10	5,16	10,46
10 wt% TCP-Al_2O_3	2,36	5,25	7	9,61	13,50
Al_2O_3	0,60	1,2	1,66	4,27	10

Table 3 Literature examples of the mechanical properties of calcium phosphates bioceramics and bone tissues

Materials	$\sigma_r^{(a)}$ (MPa)	$\sigma_c^{(b)}$ (MPa)	$\sigma_f^{(c)}$ (MPa)	References
β-TCP	4-6	-	92	(Bouslama, N *et al* 2009a) (Sakka, S *et al*, 2012)
Fap	10-14	-	-	(Ben Ayed, F *et al* 2006)
Hap	-	5.35	-	(Balcik, C et al 2007)
TCP – 75 wt% Al_2O_3	8.60	-	-	(Sakka, S *et al* 2012)
TCP – 26.52 wt% Fap	9.60	-	-	(Bouslama, N *et al* 2009a)
TCP – 26.52 wt% Fap- 5 wt% Al_2O_3	13.60	-	-	(Bouslama, N *et al* 2009b)
TCP – 33.16 wt% Fap	13.70	-	-	(Bouslama, N *et al* 2010)
Hap – TCP (40:60)	-	4.89	-	(Balcik, C et al 2007)
Al_2O_3 – 26.5 wt% Fap	21.7	-	-	(Guidara, A *et al* 2011)
Cortical bone	-	130-180	50-150	(Hench, L L 1991, 1993)
Cancellous bone	-	2-12	-	(Hench, L L 1991, 1993)

(a): Rupture strength (Brazilian test), (b): compressive strength, (c): Flexural strength.

action of several different transport mechanisms such as: surface diffusion, evaporation- condensation, grain boundary diffusion (Elliott, J. C. et al 1994). However, producing dense TCP–Al2O3 composites with a fine uniform microstructure through the sintering process does not seem to be a routine process because the β-TCP has a lower sinterability and a lower sintering temperature than those of pure alumina.

3. 3. Characterization of alumina-tricalcium phosphate composites after the sintering process

Fig. 5 shows the ^{31}P MAS-NMR spectra of the Al_2O_3-TCP composites obtained after the sintering process for 1 hour at 1550°C with different percentages of β-TCP (50 wt%, 40 wt%, 20 wt% and 10 wt%). The addition of 50 wt% Al_2O_3 to the TCP matrix shows the presence of several peaks which are assigned to the tetrahedral environment of P sites (1.03 ppm; 1.93 ppm; 3.50 ppm and 4.84 ppm) (Fig. 5a). In fact, the increasing of the percentage of alumina in the TCP matrix decreases the number of the tetrahedral phosphorus site peaks which are reduced to a large single peak with 90 wt% alumina (Fig. 5b-d). Moreover, the tetrahedral environment of the phosphorus in tricalcium phosphate is not changed after the sintering process with different percentages of alumina. But the effect of the addition of alumina to the β-TCP matrix provokes the structural rearrangement of the coordination of phosphorus in β-TCP. Similar results were previously reported in literature (Ben Ayed, F *et al* 2006, 2011; Sakka, S. *et al* 2012; Guidera, A *et al* 2011).

The ^{27}Al MAS-NMR spectra of Al_2O_3-TCP composites sintered for 1 hour at 1550°C with different percentages of β-TCP (50 wt%, 40 wt%, 20 wt% and 10 wt%) are shown in Fig. 6. The chemical shifts at 35 ppm and at 7.3 ppm indicate the presence of octahedral Al sites (Al^{VI}) and pentahedral Al sites (Al^{V}), respectively. The peak of pentahedral Al sites increases with the increase of the percentage of alumina in the Al_2O_3-TCP composites (Fig. 8b-8d). We notice especially the appearance of another octahedral Al peak at 18.6 ppm for alumina sintered with 40 wt% and 20 wt% of β-TCP (Fig. 6b-d). The aluminum in the alumina is primarily in one pentahedral Al site (35 ppm) and in one octahedral Al site (7.3 ppm) (Fig. 6e). For the alumina sintered with different percentages of β-TCP (50 wt%, 40 wt%, 20 wt% and 10 wt%), the spectra show two octahedral aluminum environments: AlO_6 at about 7.3 ppm and at 18.6 ppm (Fig. 6b-d). Indeed, the intensity of the octahedral signal at 18.6 ppm increases with the percentage of alumina. The estimated concentrations of AlO_5 and AlO_6 are reported in Table 4. During the sintering process, the aluminum in the Al_2O_3-TCP composites provokes the structural rearrangement of the coordination of aluminum. Similar results were provisionally reported by different authors (Bouslama, N *et al* 2009b; Sakka, S *et al* 2012; Guidara, A *et al* 2011). Indeed, these authors show that the coordination of the aluminum in octahedral sites was forced to change into another coordination in pentahedral sites (Guidara, A *et al* 2011). The same authors point out that the structural rearrangement of the coordination of aluminum was probably produced by the formation of calcium aluminates

which was produced after the sintering process and the reaction between calcium phosphates and alumina (Guidara, A *et al* 2011). In conclusion, the ^{31}P magic angle scanning nuclear magnetic resonance analysis of different composites reveals the presence of tetrahedral P sites, while the ^{27}Al magic angle scanning nuclear magnetic resonance analysis shows the presence of both octahedral and pentahedral Al sites.

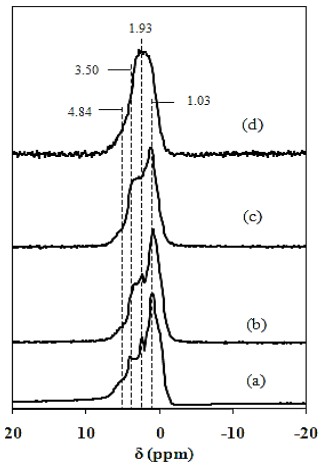

Fig. 5

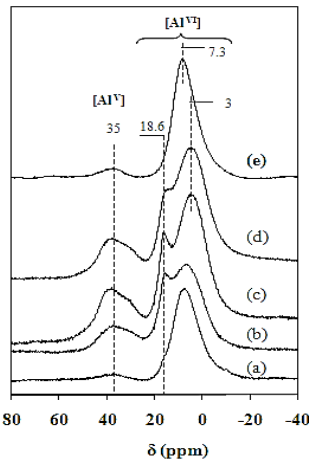

Fig. 6

Fig. 5 The ^{31}P MAS-NMR spectra of the Al_2O_3-TCP composites sintered for 1 hour at 1550°C with different percentages of β-TCP: (a) 50 wt%, (b) 40 wt%, (c) 20 wt% and (d) 10 wt

Fig. 6 The ^{27}Al MAS-NMR spectra of the Al_2O_3-TCP composites sintered for 1 hour at 1550°C with different percentages of β-TCP: (a) 50 wt%, (b) 40 wt%, (c) 20 wt%, (d) 10 wt% and (e) 0 wt%.

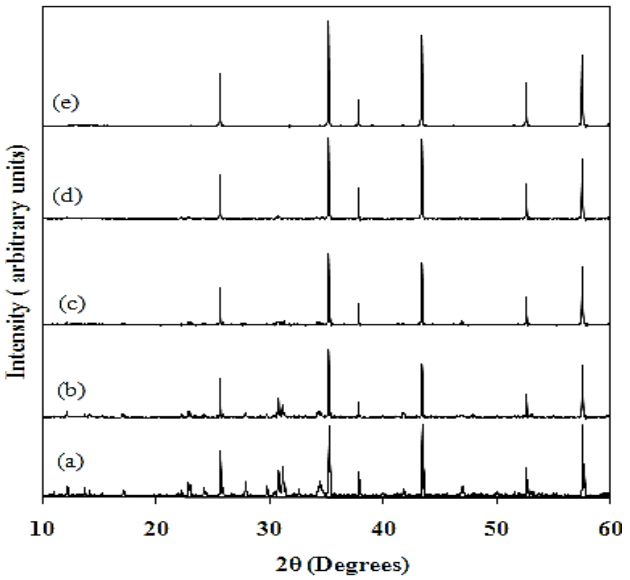

Fig. 7 The XRD patterns of the Al_2O_3-TCP composites sintered at 1550°C for 1 hour with different percentages of β-TCP: (a) 50 wt%, (b) 40 wt%, (c) 20 wt%, (d) 10 wt% and (e) 0 wt%

Fig. 7 presents XRD patterns of Al_2O_3-TCP composites sintered at 1550°C for 1 hour with different percentages of β-TCP. Besides, the spectra show the characteristic peaks of β-TCP (ICDD data file no. 70-2065) and α- Al_2O_3 (ICDD data file no. 43-1484). This analysis shows that the peak of alumina is predominant in the elaboration of any composite.

The SEM technique helps to investigate the texture and porosity of any biomaterial. Fig. 8 shows the fracture surface of the Al_2O_3-TCP composites sintered at 1550°C for 1 hour with different percentages of β-TCP. These micrographs show the coalescence between β-TCP grains produced with all the percentages of added alumina (Fig. 8a-d). The samples sintered with 50 wt%, 40 wt% and 20 wt% β-TCP present cracks and an important intragranular porosity (Fig. 8a-c). This result is a proof of the fragility of the composites elaborated with the different percentages of alumina as shown in Fig. 10a-c. In fact, the microstructure of the composites shows different cracks relative to the allotropic transformation of TCP (β to α) (Fig. 8a-c). But the intensity of the cracks in the composites decreases with the increase in the percentage of β-TCP (Fig. 8a-d). Thus, the absence of micro-cracking and the reduction of the sizes of the pores in the Al_2O_3-10 wt% TCP composites explain the increase in the rupture strength of the samples (Fig. $8d_1$-d_2). Indeed, the composites present excellent mechanical properties and a good aptitude for sinterability (Fig. $8d_1$-d_2). The SEM micrographs of the alumina sintered without β-TCP shows an intergranular porosity (Fig. 8e).

The effects of the sintering temperature on the microstructure of the Al_2O_3-10 wt% TCP composites are presented in Fig. 9. The SEM micrographs show the coalescence between the grains with the increase of the sintering temperature. At 1500°C, the samples present an important intergranular porosity (Fig. 9a). The microstructure of Al_2O_3-10 wt% TCP composites sintered at 1550°C shows a continuous phase relative to β-TCP phases and small-sized grains relative to the alumina phases (Fig. 9b). Furthermore, at 1600°C, the boundaries between grains are evident in the micrographs (marked with arrows in Fig. 9c), confirming the best mechanical resistance of Al_2O_3-10 wt% TCP composites in this temperature and with the addition of 10 wt% β-TCP (Fig. 9c). In fact, the continuous phases in addition to the formed spherical pores prove that a liquid phase has appeared at 1600°C relative probably to the allotropic transformation of the β-TCP. This similar result was observed by Bouslama and colleagues (Bouslama, N *et al* 2010).

Furthermore, the sintering behavior of the Al_2O_3-TCP composites has been studied relative to the β-TCP content. It has been shown that alumina should be used in order to prevent the β-α transition of the tricalcium phosphate during the sintering process. At any rate, the results obtained in the present work would be valuable in the performance of Al_2O_3 - TCP composites resembling bone tissue engineering (Table 3). In fact, our preliminary tests indicated that the rupture strength of Al_2O_3-TCP composites is from 2 to 14 MPa. The optimum value of

Table 4 Properties of pentahedral and octahedral Al sites in the Al_2O_3-TCP composites sintered with different percentages of β-TCP at various temperatures for 1 hour

Compounds	AlO_5 (%)	AlO_6 (Type 1) (%)	AlO_6 (Type 2) (%)
δ (ppm)	30-40	7	18
TCP - 50 wt % Al_2O_3	0.50	99.50	-
TCP - 60 wt % Al_2O_3	15.38	65.37	19.25
TCP - 80 wt % Al_2O_3	19.71	67.81	12.48
TCP- 90 wt % Al_2O_3	14.85	73.71	11.44
Al_2O_3	1.40	98.60	-

the Al_2O_3 - 10 wt% TCP composites sintered at 1600°C for one hour reached 13.5 MPa. This is true for the values of calcium phosphates fabricated by conventional techniques (Deville, S *et al* 2006) and is close to a cancellous bone (2-12 MPa) (Hench, L. L 1991,1993; Murugan, R *et al* 2005). According to the authors' best knowledge, the highest values of the mechanical characteristics for different samples are detailed in Table 3. As it can be seen from this table, the various techniques used to prepare dense sintered bioceramics affect the final density, as well as the composition of the phase and, consequently, the final mechanical properties of samples. The Al_2O_3 - 10 wt% TCP composites show high rupture strength, which is in concordance with the other results (Wang, C X *et al* 2004; Ben Ayed, F *et al* 2006, 2011; Bouslama, N *et al* 2009b, 2010 ; Sakka, S *et al* 2012). The rupture strength obtained for TCP-Al_2O_3 composites is from 2 to 14 MPa, within the values reported in the literature (Table 3). Moreover, the wide variation in the reported rupture strength of the composites is due to the synthesis route of the β-TCP powder, the size of its particle as well as to its density; it is also due to the application of different processing parameters.

At first, the objective of this work was to characterize the mechanical properties of alumina – TCP composites produced after the sintering process. A sintering stage appears to be of great importance to produce biomaterials with the required properties. Several processes occur during the sintering process of tricalcium phosphate and bioinert oxide. Firstly, the TCP powders are synthesized by solid reaction. Secondly, alumina – TCP powders are sintered for production of dense bioceramics with subsequent shrinkage of the samples. Thirdly, the mechanical properties of alumina–TCP composites are accompanied by a concurrent increase in grain size and a formation of cracks in the alumina sintered with different percentages of TCP (20 wt%, 40 wt% and 50 wt%). Besides, sintering causes the toughening and the increase of the mechanical strength of alumina–10 wt% TCP composites. An extensive study on the effect of the sintering temperature on the properties of alumina–TCP composites revealed a correlation between this parameter and density, porosity, grain size, chemical composition and strength of different composites. The degree of densification and mechanical properties of alumina–TCP composites appeared to depend on the sintering temperature. Alumina–TCP powders can be pressed and sintered up to theoretical density at 1400°C–1600°C. Processing them with higher percentage of TCP (20 wt%, 40 wt% and 50 wt%) may lead to exaggerated grain growth and formation of cracks because of the formation of α-TCP at higher temperatures. Indeed, the allotropic transformation of TCP is a function of the sintering temperature. The presence of cracks in the alumina–TCP composites is reported to inhibit the mechanical properties. A definite correlation between mechanical strength and grain size in sintered alumina–TCP composites was found: the strength started to decrease at lower sintering temperature and with higher percentage of

TCP (20 wt%, 40 wt% and 50 wt%). The sintering process of alumina – 10 wt% TCP composites makes it possible to decrease the grain size and achieve higher densities. This leads to finer microstructures, higher thermal stability of alumina–10 wt% TCP composites and subsequently better mechanical properties of the prepared bioceramics composites. The mechanical properties of alumina – TCP composites is from 2 to 14 MPa. Generally, the mechanical properties of samples increase with the decrease in grain size. In fact, the mechanical strength of alumina–10 wt% TCP composites reaches a maximum value with the decrease in the size of the grains of composites. The optimum measured value of the strength of the alumina–10 wt% TCP composites was 13.5 MPa. This value is compared to those of cancellous bone. Similar values for porous HAp are in the ranges of 2-10 MPa (Suchanek, W L *et al* 1998). Generally, variations of mechanical properties of samples are caused by a statistical nature of the strength distribution, influence of remaining microporosity, grain size, presence of impurities and Ca/P ratio (Suchanek, W L *et al* 1998).

In conclusion, an interfacial reaction between β-TCP and alumina has been studied in the nanocomposites of Al_2O_3-TCP. It was found that the alumina did not completely react with the β-TCP and did not form calcium aluminates. Moreover, it has been shown that the alumina prevents the formation of cracks in the microstructure of composites containing 10 wt% of β-TCP. The mechanical characteristics should be taken into consideration in order to better assess the relationship between the processing conditions, the microstructural design as well as the mechanical response.

Conclusions

The biomaterials of alumina-tricalcium phosphate composites have been characterized by using MAS NMR, XRD and SEM analysis after the sintering process. The effect of β-TCP additive on the alumina matrix was obser-

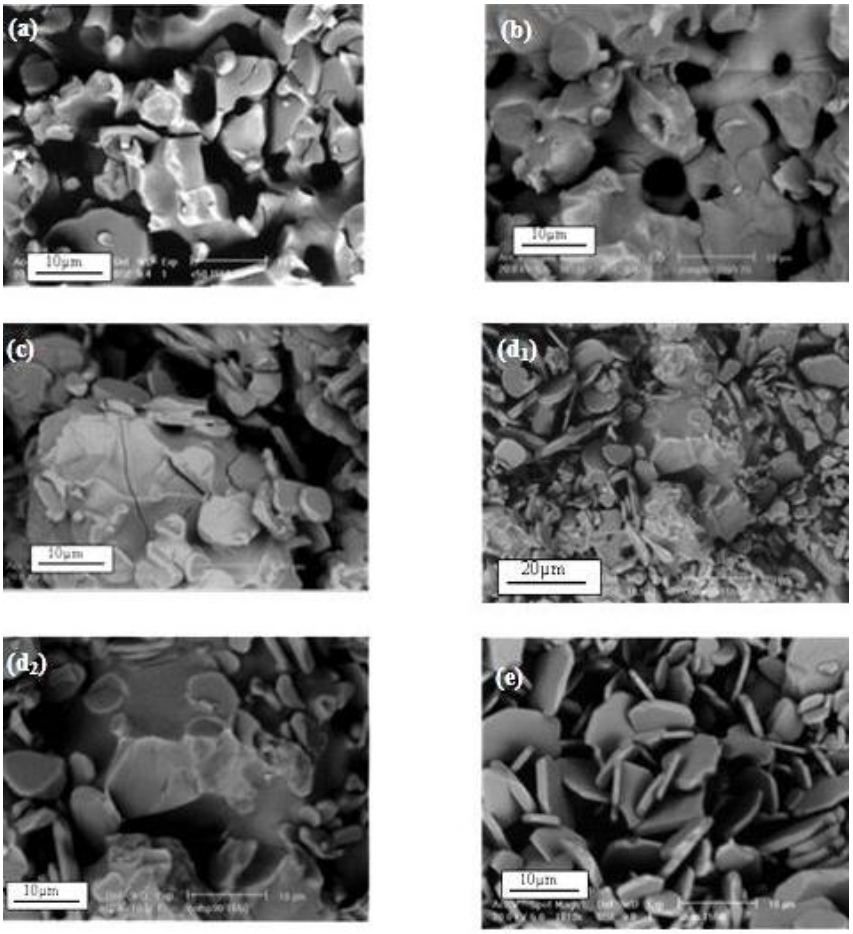

Fig. 8 The SEM micrographs of the Al_2O_3 - TCP composites sintered at 1550°C for 1 hour with different percentages of β-TCP: (a) 50 wt%, (b) 40 wt%, (c) 20 wt%, (d_1-d_2) 10 wt% and (e) 0 wt%.

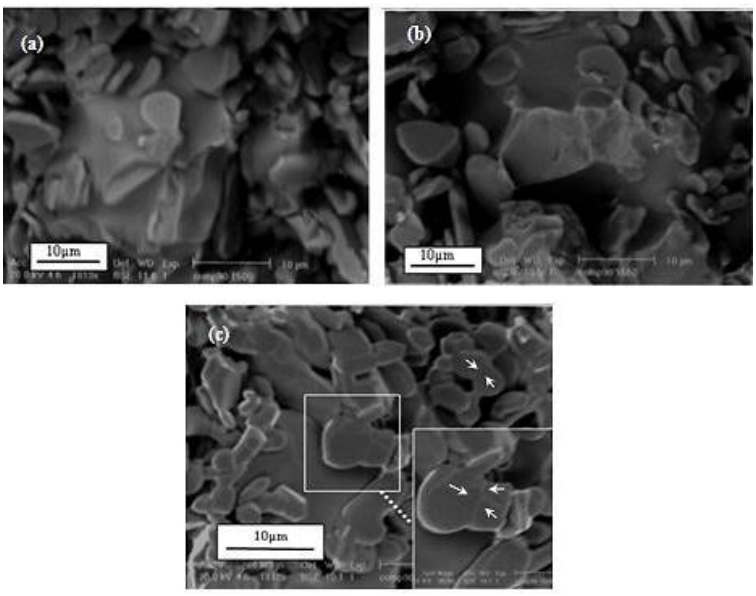

Fig. 9 The SEM micrographs of the Al2O3-10 wt% TCP composites sintered for 1 hour at: (a) 1500°C, (b) 1550°C and (c) 1600°C

-ved in different thermal analyses: dilatometry analysis and DTA analysis. The mechanical properties have been investigated by the Brazilian test. This investigation has allowed us to define the sintering temperature and the percentage of added alumina for which β-TCP should have an optimal densification and better mechanical

properties. This study has also allowed us to summarize the effect of the sintering temperature and the length of sintering time on the mechanical properties of the Al_2O_3-TCP composites. The produced Al_2O_3-TCP composites with different percentages of β-TCP (50 wt%; 40 wt%; 20 wt% and 10 wt%) exhibited much better mechanical properties than the reported values of β-TCP without alumina. The Al_2O_3-TCP composites showed a higher rupture strength at 1600°C, which certainly increased with the alumina content and reached the optimum value with 90 wt%. However, no cracks were observed in the microstructure of the composites which contained this percentage of alumina. This is due to the allotropic transformation of the tricalcium phosphate. The partial or reversal transformation of tricalcium phosphate (β to α or α to α') during the cooling period could induce a residual stress within the dense bioceramics, marking it much more brittle. Accordingly, the optimum performance of alumina-tricalcium phosphate composites achieved 13.5 MPa. Furthermore, the best mechanical properties of the composites were obtained after the sintering process at 1600°C for 1 hour. With different weight rations of alumina : tricalcium phosphate (50:50, 60:40 and 80:20), the performance of the composites was hindered by the formation of both cracks and intragranular porosity.

6. References

ASTM C496, (1984), Standard test method for splitting tensile strength of cylindrical concrete specimens. *In: Annual Book of ASTM, Standards*, vol. 0.042. ASTM, Philadelphia, p. 336.

Balcik, C., Tokdemir, T., Senkoylo, A., Koc, N., Timucin, M., Akin, S., Korkusuz, P., Korkusuz, F.,(2007), Early weight bearing of porous HA/TCP (60/40) ceramics in vivo: a longitudinal study in a segmental bone defect model of rabbit. *Acta Biomaterialia*, 3, 985-996.

Ben Ayed, F., Bouaziz, J., Bouzouita, K., (2000), Pressureless sintering of fluorapatite under oxygen atmosphere, *Journal of the European Ceramic Society*, 20, 1069.

Ben Ayed, F., Bouaziz, J., Khattech, I., Bouzouita, K., (2001), Produit de solubilité apparent de la fluorapatite frittée, *Annales de Chimie - Science des Materiaux*, 26 (6), 75.

Ben Ayed, F., Chaari, K., Bouaziz, J., Bouzouita, K., (2006), Frittage du phosphate tricalcique, *Comptes Rendus Physique*, 7, 825.

Ben Ayed, F., Bouaziz, J., (2008), Sintering of tricalcium phosphate–fluorapatite composites by addition of alumina, *Ceramics International*, 34, 1885-1892

Ben Ayed, F., (2011), Elaboration and characterization of calcium phosphate biomaterial for biomedical application, *in Tech, Biomaterials - Physics and Chemistry*, ISBN 978-953-307-418-4, Croatia, pp.357-374.

Bouslama, N., Ben Ayed, F., Bouaziz, J., (2009a), Sintering and mechanical properties of tricalcium phosphate–fluorapatite composites, *Ceramics International*, 35, 1909-1917.

Bouslama, N., Ben Ayed, F., Bouaziz, J., (2009b), Mechanical properties of tricalcium phosphate-fluorapatite-alumina composites, *Physics Procedia*, 2, 1441-1448.

Bouslama, N., Ben Ayed, F., Bouaziz, J., (2010), Effect of fluorapatite additive on densification and mechanical properties of tricalcium phosphate, *Journal of the Mechanical Behavior of Biomedical Materials*, 3, 2-13.

Brunauer, S., Emmet ,P.H., Teller, J., (1938), Adsorption of Gases in Multimolecular Layers, *Journal of the American Chemical Society*, 60, 310.

Chu, T. M.G., Orton, D.G., Hollister, S.J., Feinberg, S.E., Halloran, J.W., (2002), Mechanical and in vivo performance of hydroxyapatite implants with controlled architectures, *Biomaterials*, 23, 1283–93.

DeSilva, G. L., Fritzler, A., DeSilva, S. P., (2007), Antibiotic-impregnated cement spacer for bone defects of the forearm and hand, *Techniques in Hand & Upper Extremity Surgery*, 11, 163–7.

Destainville, A., Champion, E., Bernache – Assolant, D., (2003), Synthesis, characterization and thermal behavior of apatitic tricalcium phosphate, *Materials Chemistry and Physics*, 80, 269-277.

Deville, S., Saiz, E., Nalla, R. K., Tomsia, A. P., (2006), Freezing as a path to build complex composites, Science, 311 (5760), 515-518.

Elliott, J. C., (1994), Structure and Chemistry of the Apatite and Other Calcium Orthophosphates, *Elsevier Science B.V*, Amsterdam.

Gaasbeek, R. D., Toonen, H.G., Van Heerwaarden, R.J., Buma, P., (2005), Mechanism of bone incorporation of β-TCP bone substitute in open wedge tibial osteotomy in patients, *Biomaterials*, 26, 6713–6719.

Guha, A. K., Singh, S., Kumarresan, R., Nayar, S., Sinha, A., (2009), Mesenchymal cell response to nanosized biphasic calcium phosphate composites, *Colloids and Surfaces B: Biointerfaces*, 73, 146-51.

Guidara, A., Chaari, K., Bouaziz, J., (2011), Elaboration and Characterization of Alumina -Fluorapatite Composites. *Journal of Biomaterials and Nanobiotechnology*, 2, 103-113.

Gutierres, M., Dias, A. G., Lopes, M. A., Hussain, N. S., Cabral, A. T., Almeid L., (2007), Opening wedge high tibial osteotomy using 3D biomodelling Bone like macroporous struc- tures: case report, *Journal of Materials Science: Materials in Medicine*, 7 (18), 2377–2382.

Hench, L. L., (1991), Bioceramics: From concept to clinic, *Journal of the American Ceramic Society*, Vol.74, pp.1487-1510.

Hench, L. L., Wilson, J., (1993), An Introduction to Bioceramics. *Advanced series in ceramics*. Vol. 1. World Scientific, Singapore.

Hoell, S., Suttmoeller, J., Stoll, V., Fuchs, S., Gosheger, G., (2005), The high tibial osteotomy, open versus closed wedge, a comparison of methods in 108 patients. *Archives of Orthopaedic and Trauma Surgery*, 125, 638–643.

ISRM., (1978), Suggested methods for determining tensile strength of rock materials. *International Journal of Rock Mechanics and Mining Sciences & Geomechanics Abstracts*,15, pp.99.

Jensen, S. S., Broggini, N., Hjorting-Hansen, E., Schenk, R., Buser, D., (2006), Bone healing and graft resorption of autograft, anorganic bovine bone and beta-tricalcium phosphate.A histologic and histomorphometric study in the mandibles of minipigs, *Clinical Oral Implants Research*, 17, 237–243.

Landi, E., Tampieri, A., Celotti, G., Sprio, S., (2000), Densification behaviour and mechanisms of synthetic hydroxyapatites, *Journal of the European Ceramic Society*, 20, 2377.

Langstaff, S. D., Sayer, M., Smith, T.J. N., Pugh, S.M., (2001), Resorbable bioceramics based on stabilized calcium phosphates. Part II: evaluation of biological response. *Biomaterials*, 22, 135–50.

LeGeros, R. Z., (1991), Calcium phosphates in oral biology and medicine, Basel: Karger, 201.

Murugan, R., Ramakrishna, S., (2005), Development of nanocomposites for bone grafting, *Composites Science and Technology*, 65, 2385-2406.

Sakka, S., Ben Ayed, F., Bouaziz, J., (2012), Mechanical properties of tricalcium phosphate alumina composites. *IOP Conf. Series: Materials Science and Engineering*, 28, 012028.

Schnettler, R., Stahl, J.P., Alt, V., Pavlidis, T., Dingeldein, E., Wenisch, S., (2004), Calcium phosphate-based bone substitutes, *European Journal of Trauma*, 4, 219–29.

Sellami, I., Ben Ayed, F., Bouaziz, J., (2012), Effect of fluorapatite additive on the mechanical properties of tricalcium phosphate-zirconia composites, *IOP Conf. Series: Materials Science and Engineering*, 28, 012029.

Suchanek, W. L., Yoshimura, M., (1998), Processing and properties of hydroxyapatite based bio- materials for use as hard tissue replacement implants, *Journal of Materials Research*, 13, 94–117.

Tamai, N., Myoui, A., Tomita, T., Nakase, T., Tanaka, J., Ochi, T., (2002), Novel hydroxyapatite ceramics with an interconnective porous structure exhibit superior osteoconduction in vivo, *Journal of Biomedical Materials Research*, 59, 110–7.

Wang, C. X., Zhou, X., Wang, M., (2004), Influence of sintering temperatures on hardness and Young's modulus of tricalcium phosphate bioceramic by nanoindentation technique. *Materials Characterization*, 52, 301.